Inorganic Chemistry

Article

Assembly of the Highest Connectivity Wells-Dawson Polyoxometalate Coordination Polymer: the Use of Organic Ligand Flexibility

Ai-xiang Tian,[†] **Jun Ying,**[†] **Jun Peng,**[*,†] **Jing-quan Sha,**[†] **Zhan-gang Han,**[†] **Jian-fang Ma,**[†] **Zhong-min Su,**[†] **Ning-hai Hu,**[‡] **and Heng-qing Jia**[‡]

Key Laboratory of Polyoxometalate Science of Ministry of Education, Faculty of Chemistry, Northeast Normal University, Changchun, Jilin 130024, P.R. China, and, Changchun Institute of Applied Chemistry, Chinese Academy of Science, Changchun 130022, P.R. China

Through tuning the length of flexible bis(triazole) ligands and different metal ion coordination geometries, four Wells-Dawson polyoxoanion-based hybrid compounds, $[Cu_6(btp)_3(P_2W_{18}O_{62})] \cdot 3H_2O$ (**1**) (btp = 1,3-bis(1,2,4-triazol-1-y1)propane), $[Cu_6(btb)_3((P_2W_{18}O_{62})] \cdot 2H_2O$ (**2**), $[Cu_3(btb)_6(P_2W_{18}O_{62})] \cdot 6H_2O$ (btb = 1,4-bis(1,2,4-triazol-1-y1)butane) (**3**), and $[Cu_3(btx)_{5.5}((P_2W_{18}O_{62})] \cdot 4H_2O$ (btx = 1,6-bis(1,2,4-triazol-1-y1)hexane) (**4**), were synthesized and structurally characterized. In compound **1**, the metal-organic motif exhibits a ladder-like chain, which is further fused by the ennead-dentate $[P_2W_{18}O_{62}]^{6-}$ anions to construct a 3D structure. In compound **2**, the metal-organic motif exhibits an interesting Cu−btb grid layer, and the ennead-dentate polyoxoanions are sandwiched by two Cu−btb layers to construct a 3D structure. Compound **3** exhibits a $(4^2 \cdot 6^2 \cdot 8^2)$ 3D Cu−btb framework with square and hexagonal channels arranged alternately. The hexa-dentate polyoxoanions incorporate only into the hexagonal channels. In compound **4**, there exist two sets of $(6^1 \cdot 10^2)_2(6^1 \cdot 8^2 \cdot 10^3)$ 3D Cu−btx frameworks to generate a 2-fold interpenetrated structure into which the penta-dentate polyoxoanions are inserted to construct a 3D structure. The structural analyses reveal that the length of flexible bis(triazole) ligands and metal ion coordination geometries have a synergic influence on the structures of this series. To our knowledge, they have the highest connectivity for the Wells-Dawson polyoxometalate coordination polymers to date.

Introduction

Hybrid inorganic–organic compounds are a new generation of solid-state materials that have promising applications in gas storage, catalysis, and porous materials owing to their chemical and structural diversity.[1–3] In this field, a remarkable branch is the combination of polyoxometalates (POMs) with metal-organic frameworks (MOFs) to construct such inorganic–organic compounds[4] which brings together the merits of each, such as structural diversity with unique framework topologies and the combination of the unique physical and chemical properties of POMs with the feature of MOFs.[5] A main feature of POMs as inorganic ligands is their potential offer of multiple coordination sites, but their relatively weak coordination ability makes it an arduous and

* To whom correspondence should be addressed. E-mail: jpeng@nenu.edu.cn. Telephone: +86 43185099667. Fax: +86 43185098768.
† Northeast Normal University.
‡ Chinese Academy of Science.

(1) (a) Cheetham, A. K.; Rao, C. N. R.; Feller, R. K. *Chem. Commun.* **2006**, 4780. (b) Rowsell, J. L. C.; Millward, A. R.; Park, K. S.; Yaghi, O. M. *J. Am. Chem. Soc.* **2004**, *126*, 5666. (c) Rowsell, J. L. C.; Yaghi, O. M. *Angew. Chem., Int. Ed.* **2005**, *44*, 4670. (d) Rood, J. A.; Noll, B. C.; Henderson, K. W. *Inorg. Chem.* **2006**, *45*, 5521. (e) Spencer, E. C.; Howard, J. A. K.; McIntyre, G. J.; Rowsell, J. L. C.; Yaghi, O. M. *Chem. Commun.* **2006**, 278.
(2) (a) Fujita, M.; Kwon, Y. J.; Washizu, S.; Ogura, K. *J. Am. Chem. Soc.* **1994**, *116*, 1151. (b) Wu, C.-D.; Hu, A.; Zhang, L.; Lin, W.-B. *J. Am. Chem. Soc.* **2005**, *127*, 8940. (c) Clearfield, A.; Wang, Z.-K. *J. Chem. Soc., Dalton Trans.* **2002**, 2937.

(3) (a) Holman, K. T.; Pivovar, A. M.; Swift, J. A.; Ward, M. D. *Acc. Chem. Res.* **2001**, *34*, 107. (b) Pan, L.; Olson, D. H.; Ciemnolonski, L. R.; Heddy, R.; Li, J. *Angew. Chem., Int. Ed.* **2006**, *45*, 616. (c) Kitagawa, S.; Kitaura, R.; Noro, S. *Angew. Chem., Int. Ed.* **2004**, *43*, 2334. (d) Sun, Y.-Q.; Zhang, J.; Chen, Y.-M.; Yang, G.-Y. *Angew. Chem., Int. Ed.* **2005**, *44*, 5814.
(4) (a) Botar, B.; Kögerler, P.; Hill, C. L. *Inorg. Chem.* **2007**, *46*, 5398. (b) Long, D.-L.; Burkholder, E.; Cronin, L. *Chem. Soc. Rev.* **2007**, *36*, 105. (c) An, H.-Y.; Wang, E.-B.; Xiao, D.-R.; Li, Y.-G.; Su, Z.-M.; Xu, L. *Angew. Chem., Int. Ed.* **2006**, *45*, 904. (d) Chang, W.-J.; Jiang, Y.-C.; Wang, S.-L.; Lii, K.-H. *Inorg. Chem.* **2006**, *45*, 6586. (e) Mialane, P.; Dolbecq, A.; Sécheresse, F. *Chem. Commun.* **2006**, 3477. (f) Mal, S. S.; Nsouli, N. H.; Dickman, M. H.; Kortz, U. *J. Chem. Soc., Dalton Trans.* **2007**, 2627. (g) Wei, M.-L.; He, C.; Hua, W.-J.; Duan, C.-Y.; Li, S.-H.; Meng, Q.-J. *J. Am. Chem. Soc.* **2006**, *128*, 13318. (h) Reinoso, S.; Dickman, M. H.; Matei, M. F.; Kortz, U. *Inorg. Chem.* **2007**, *46*, 4383.

appealing task for coordination chemists to assemble a variety of POMs by covalently grafting onto MOFs with high dimensionality. Two effective strategies are currently explored, namely, to select the coordination modes of organic ligands[6] and to tune the coordination environments of the transition metal ions.[7] Extensive investigations indicate that polyoxoanion templates,[7f,8] metal ion coordination geometries, and flexibility of organic ligands all influence the high-dimensional assembly of POM coordination polymers.

Notably, in the area of MOF polymers, the introduction of flexible ligands has become popular.[9] The flexible ligands are excellent synthons for the construction of functional porous coordination polymer materials; especially attractive are those that have a dynamic crystal transformation property.[10] Their flexibility and conformational freedom allow them to conform to the coordination environment of the metal ions and POM templates. In our previous work, we introduced the flexible 1,1′-(1,4-butanediyl)bis(imidazole) (bbi) ligand into the polyoxovanadate systems.[7f] The bbi molecule has two N donors as coordination sites. However, compared with flexible imidazole and other bipyridyl ligands,[11] the flexible derivatives of 1,2,4-triazole have more advantages:[12] (i) The 1,2,4-triazole group, with three N donors, is an integration of the coordination geometry of both imidazoles and pyrazoles to provide more potential coordination sites. (ii) This kind of ligand exhibits strong and typical coordination capacity, acting as bridging ligands to construct

the MOF high-dimensional structures. This feature makes them attractive for designing new inorganic–organic polymers with interesting structures. In our continuous work of introducing flexible organic ligands into the POM system, we chose 1,2,4-triazole based N-heterocyclic molecules, 1,3-bis(1,2,4-triazol-1-y1)propane (btp), 1,4-bis(1,2,4-triazol-1-y1)butane (btb), and 1,6-bis(1,2,4-triazol-1-y1)hexane (btx) as organic ligands, which exhibit different steric hindrance and coordination diversity.

On the other hand, compared with the other well-known POMs, such as Keggin,[13] Anderson,[14] and Lindqvist,[15] the Wells-Dawson type anions[16] possess unique properties: (i) Given a larger molecular volume with 18 terminal O atoms and 36 μ_2-O atoms, the Wells-Dawson type anion offers smarter potential coordination sites to link metal-organic units, making the formation of high-dimensional framework easier. (ii) There are two categories of M atoms (M = W/Mo) in a Wells-Dawson anion, that is, 6 polar and 12 equatorial M atoms, which create different environments to bring about unsymmetrical structures. Polyoxometalate chemists are keen to extend the Wells-Dawson POM coordination polymer family, but only one 3D POM coordination polymer based on Wells-Dawson type anions has been reported up to now;[17] furthermore, the highest number of connecting sites of the POM anions is only four.[16d,i,17]

In this work, we introduce the flexible organic ligands btp, btb, and btx into the Wells-Dawson POM system, aiming at obtaining novel architectures of POM coordination polymers with a combination of flexibility and robustness. Herein we report four new inorganic–organic hybrid compounds, [Cu$_6$(btp)$_3$(P$_2$W$_{18}$O$_{62}$)]·3H$_2$O (**1**), [Cu$_6$(btb)$_3$((P$_2$W$_{18}$O$_{62}$)]·2H$_2$O (**2**), [Cu$_3$(btb)$_6$(P$_2$W$_{18}$O$_{62}$)]·6H$_2$O (**3**), and [Cu$_3$(btx)$_{5.5}$((P$_2$W$_{18}$O$_{62}$)]·4H$_2$O (**4**) (Scheme 1), where the polyoxoanions act as ennead- (**1** and **2**), hexa- (**3**), and penta- (**4**) dentate inorganic ligands, respectively. The influences of flexible

(5) (a) Streb, C.; Ritchie, C.; Long, D.-L.; Kögerler, P.; Cronin, L. *Angew. Chem., Int. Ed.* **2007**, *46*, 7579. (b) Song, Y.-F.; Long, D.-L.; Cronin, L. *Angew. Chem., Int. Ed.* **2007**, *46*, 3900.

(6) (a) Hagrman, P. J.; LaDuca, R. L.; Koo, H. J.; Rarig, R.; Haushalter, R. C.; Whangbo, M. H.; Zubieta, J. *Inorg. Chem.* **2000**, *39*, 4311. (b) Ren, Y.-P.; Kong, X.-J.; Hu, X.-Y.; Sun, M.; Long, L.-S.; Huang, R.-B.; Zheng, L.-S. *Inorg. Chem.* **2006**, *45*, 4016.

(7) (a) Hagrman, P. J.; Zubieta, J. *Inorg. Chem.* **2000**, *39*, 5218. (b) Rarig, R. S.; Zubieta, J. *J. Chem. Soc., Dalton Trans.* **2001**, 3446. (c) Burkholder, E.; Golub, V.; O'Connor, J. C.; Zubieta, J. *Inorg. Chem.* **2004**, *43*, 7014. (d) Li, S.-L.; Lan, Y.-Q.; Ma, J.-F.; Yang, J.; Wang, X.-H.; Su, Z.-M. *Inorg. Chem.* **2007**, *46*, 8283. (e) Shi, Z.-Y.; Peng, J.; Gómez-García, C. L.; Benmansour, S.; Gu, X.-J. *J. Solid State Chem.* **2006**, *179*, 253. (f) Dong, B.-X.; Peng, J.; Gómez-García, C. L.; Benmansour, S.; Jia, H.-Q.; Hu, N.-H. *Inorg. Chem.* **2007**, *46*, 5933.

(8) (a) Hagrman, D.; Hagrman, P. J.; Zubieta, J. *Angew. Chem., Int. Ed.* **1999**, *38*, 3165. (b) Inman, C.; Knaust, J. M.; Keller, S. W. *Chem. Commun.* **2002**, 156. (c) Knaust, J. M.; Inman, C.; Keller, S. W. *Chem. Commun.* **2004**, 492. (d) Ishii, Y.; Takenaka, Y.; Konishi, K. *Angew. Chem., Int. Ed.* **2004**, *43*, 2702.

(9) (a) Wang, X.-L.; Qin, C.; Wang, E.-B.; Su, Z.-M. *Chem.—Eur. J.* **2006**, *12*, 2680. (b) Wang, Y.; Ding, B.; Cheng, P.; Liao, D.-Z.; Yan, S.-P. *Inorg. Chem.* **2007**, *46*, 2002. (c) Yi, L.; Yang, X.; Lu, T.-B.; Cheng, P. *Cryst. Growth. Des.* **2005**, *5*, 1215. (d) Yi, L.; Ding, B.; Zhao, B.; Cheng, P.; Liao, D.-Z.; Yan, S.-P.; Jiang, Z.-H. *Inorg. Chem.* **2004**, *43*, 33. (e) Liu, Y.-Y.; Ma, J.-F.; Yang, J.; Su, Z.-M. *Inorg. Chem.* **2007**, *46*, 3027. (f) Bu, X.-H.; Chen, W.; Lu, S.-L.; Zhang, R.-H.; Liao, D.-Z.; Bu, W.-M.; Shionoya, M.; Brisse, F.; Ribas, J. *Angew. Chem., Int. Ed.* **2001**, *40*, 3201. (g) Bu, X.-H.; Chen, W.; Hou, W.-F.; Du, M.; Zhang, R.-H.; Brisse, F. *Inorg. Chem.* **2002**, *41*, 3477. (h) Bu, X.-H.; Xie, Y.-B.; Li, J.-R.; Zhang, R.-H. *Inorg. Chem.* **2003**, *42*, 7422.

(10) Kitagawa, S.; Kitaura, R.; Noro, S.-I. *Angew. Chem., Int. Ed.* **2004**, *43*, 2334.

(11) (a) Qu, X.-S.; Xu, L.; Gao, G.-G.; Li, F.-Y.; Yang, Y.-Y. *Inorg. Chem.* **2007**, *46*, 4775. (b) Qu, X.-S.; Xu, L.; Li, F.-Y.; Gao, G.-G.; Yang, Y.-Y. *Inorg. Chem. Commun.* **2007**, *10*, 1404.

(12) (a) Beckmann, U.; Brooker, S. *Coord. Chem. Rev.* **2003**, *245*, 17. (b) Haasnoot, J. G. *Coord. Chem. Rev.* **2000**, *200–202*, 131. (c) Wang, X.-L.; Qin, C.; Wang, E.-B.; Su, Z.-M.; Li, Y.-G.; Xu, L. *Angew. Chem., Int. Ed.* **2006**, *45*, 7411. (d) Wang, X.-L.; Qin, C.; Wang, E.-B.; Su, Z.-M. *Chem. Commun.* **2007**, 4245.

(13) (a) Yokoyama, A.; Kojima, T.; Ohkubo, K.; Fukuzumi, S. *Chem. Commun.* **2007**, 3997. (b) Uehara, K.; Nakao, H.; Kawamoto, R.; Hikichi, S.; Mizuno, N. *Inorg. Chem.* **2006**, *45*, 9448. (c) Li, Y.-G.; Dai, L.-M.; Wang, Y.-H.; Wang, X.-L.; Wang, E.-B.; Su, Z.-M.; Xu, L. *Chem. Commun.* **2007**, 2593.

(14) (a) Shivaiah, V.; Das, K. S. *Inorg. Chem.* **2005**, *44*, 8846. (b) An, H.-Y.; Li, Y.-G.; Wang, E.-B.; Xiao, D.-R.; Sun, C.-Y.; Xu, L. *Inorg. Chem.* **2005**, *44*, 6062. (c) Cao, R.-G.; Liu, S.-X.; Xie, L.-H.; Pan, Y.-B.; Cao, J.-F.; Ren, Y.-H.; Xu, L. *Inorg. Chem.* **2007**, *46*, 3541.

(15) (a) Kang, J.; Xu, B.-B.; Peng, Z.-H.; Zhu, X.-D.; Wei, Y.-G.; Powell, D. R. *Angew. Chem., Int. Ed.* **2005**, *44*, 2. (b) Bar-Nahum, I.; Narasimhulu, K. V.; Weiner, L.; Neumann, R. *Inorg. Chem.* **2005**, *44*, 4900. (c) Xia, Y.; Wei, Y.-G.; Wang, Y.; Guo, H.-Y. *Inorg. Chem.* **2005**, *44*, 9823.

(16) (a) Yan, B.-B.; Xu, Y.; Bu, X.-H.; Goh, N. K.; Chia, L. S.; Stucky, G. D. *J. Chem. Soc., Dalton Trans.* **2001**, 2009. (b) Niu, J.-Y.; Guo, D.-J.; Zhao, J.-W.; Wang, J.-P. *New. J. Chem.* **2004**, *28*, 980. (c) Niu, J.-Y.; Guo, D.-J.; Wang, J.-P.; Zhao, J.-W. *Cryst. Growth Des.* **2004**, *4*, 241. (d) Dong, B.-X.; Peng, J.; Chen, Y.-H.; Zhang, P.-P.; Tian, A.-X.; Chen, J. *J. Mol. Struct.* (2007), doi: 10.1016/j.molstruc. 2007.04.003. (e) Fan, L.-L.; Wang, E.-B.; Li, Y.-G.; An, H.-Y.; Xiao, D.-R.; Wang, X.-L. *J. Mol. Struct.* **2007**, *841*, 28. (f) Jin, H.; Wang, X.-L.; Qi, Y.-F.; Wang, E.-B. *Inorg. Chim. Acta* **2007**, *360*, 3347. (g) Tian, A.-X.; Han, Z.-G.; Peng, J.; Dong, B.-X.; Sha, J.-Q.; Li, B. *J. Mol. Struct.* **2007**, *832*, 117. (h) Wang, J.-P.; Wang, W.; Niu, J.-Y. *Inorg. Chem. Commun.* **2007**, *10*, 520. (i) Soumahoro, T.; Burkholder, E.; Ouellette, W.; Zubieta, J. *Inorg. Chim. Acta* **2005**, *358*, 606.

(17) Sha, J.-Q.; Wang, C.; Peng, J.; Chen, J.; Tian, A.-X.; Zhang, P.-P. *Inorg. Chem. Commun.* **2007**, *10*, 1321.

Scheme 1. Experimental Routes for Compounds **1–4**
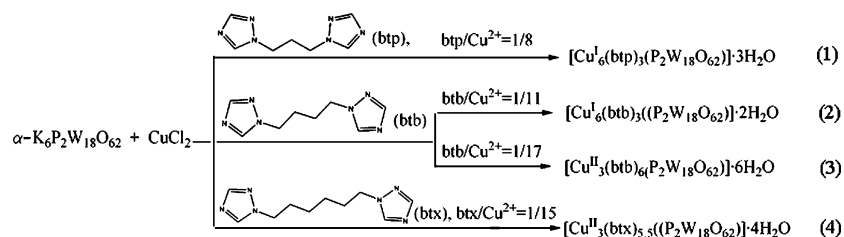
bis(triazole) ligands and metal ion coordination geometries on the high-dimensional structures are discussed.

Experimental Section

Materials and General Methods. All reagents and solvents for syntheses were purchased from commercial sources and were used as received. The α-K$_6$P$_2$W$_{18}$O$_{62}$·15H$_2$O was prepared according to the literature method[18] and verified by infrared (IR) spectrum. Elemental analyses (C, H, and N) were performed on a Perkin-Elmer 2400 CHN elemental analyzer. The IR spectra were obtained on Alpha Centauri Fourier transform IR (FT-IR) spectrometer with KBr pellet in the 400–4000 cm^{-1} region. The thermogravimetric analyses (TGA) were carried out in N$_2$ on a Perkin-Elmer DTA 1700 differential thermal analyzer with a rate of 10.00 °C/min. The X-ray powder diffraction (XRPD) patterns were recorded on a Siemens D5005 diffractometer with Cu Kα (λ = 1.5418 Å) radiation. Electrochemical measurements were performed with a CHI 660b electrochemical workstation. A conventional three-electrode system was used. Ag/AgCl (3 M KCl) electrode was used as a reference electrode, and a Pt wire as a counter electrode. Chemically bulk-modified carbon-paste electrodes (CPEs) were used as the working electrodes.

Synthesis of [Cu$_6$(btp)$_3$(P$_2$W$_{18}$O$_{62}$)]·3H$_2$O (1). A mixture of α-K$_6$P$_2$W$_{18}$O$_{62}$·15H$_2$O (0.35 g, 0.072 mmol), CuCl$_2$ (0.25 g, 1.86 mmol), and btp (0.041 g, 0.23 mmol) was dissolved in 10 mL of distilled water at room temperature. When the pH value of the mixture was adjusted to about 4.6 with 1.0 mol L^{-1} NaOH, the suspension was put into a Teflon-lined autoclave and kept under autogenous pressure at 160 °C for 5 days. After slow cooling to room temperature, red brown block crystals were filtered and washed with distilled water (40% yield based on W). Anal. Calcd for C$_{21}$H$_{36}$Cu$_6$N$_{18}$O$_{65}$P$_2$W$_{18}$ (5332.9): C 4.73, H 0.68, N 4.73. Found: C 4.69, H 0.70, N 4.69. IR (solid KBr pellet, cm^{-1}): 3848 (w), 3748 (w), 3429 (s), 3115 (w), 1698 (m), 1642 (m), 1527 (s), 1429 (w), 1357 (w), 1294 (w), 1217 (w), 1140 (w), 1089 (s), 955 (m), 905 (m), 773(s).

Synthesis of [Cu$_6$(btb)$_3$((P$_2$W$_{18}$O$_{62}$)]·2H$_2$O (2). A mixture of α-K$_6$P$_2$W$_{18}$O$_{62}$·15H$_2$O (0.21 g, 0.043 mmol), CuCl$_2$ (0.35 g, 2.6 mmol), and btb (0.046 g, 0.24 mmol) was dissolved in 10 mL of distilled water at room temperature. When the pH value of the mixture was adjusted to about 4.5 with 1.0 mol L^{-1} NaOH, the suspension was put into a Teflon-lined autoclave and kept under autogenous pressure at 160 °C for 5 days. After slow cooling to room temperature, red brown block crystals were filtered and washed with distilled water (40% yield based on W). Anal. Calcd for C$_{24}$H$_{40}$Cu$_6$N$_{18}$O$_{64}$P$_2$W$_{18}$ (5357): C 5.38, H 0.75, N 4.70. Found: C 5.34, H 0.77, N 4.73. IR (solid KBr pellet, cm^{-1}): 3856 (w), 3739 (m), 3431 (s), 3129 (w), 2923 (w), 1685 (m), 1650 (s), 1537 (s), 1455 (m), 1357 (w), 1294 (w), 1153 (w), 1088 (s), 954 (w), 911 (w), 778 (s), 662 (w), 583 (w), 515 (w).

Synthesis of [Cu$_3$(btb)$_6$(P$_2$W$_{18}$O$_{62}$)]·6H$_2$O (3). Compound **3** was prepared similarly to compound **2**, except for changing the weight of the btb ligand (0.03 g, 0.16 mmol). Blue block crystals were filtered and washed with distilled water (60% yield based on W). Anal. Calcd for C$_{48}$H$_{84}$Cu$_3$N$_{36}$O$_{68}$P$_2$W$_{18}$ (5815.09): C 9.91, H 1.44, N 8.67. Found: C 9.87, H 1.46, N 8.71. IR (solid KBr pellet, cm^{-1}): 3841 (w), 3748 (w), 3415 (s), 3129 (w), 2952 (w), 1631 (s), 1527 (s), 1445 (m), 1380 (w), 1287 (m), 1209 (w), 1130 (m), 1090 (m), 953 (m), 905 (w), 782 (s), 659 (w), 519 (w).

Synthesis of [Cu$_3$(btx)$_{5.5}$((P$_2$W$_{18}$O$_{62}$)]·4H$_2$O (4). Compound **4** was prepared similarly to compound **3**, but the btx ligand was used instead of the btb ligand (0.037 g, 0.17 mmol). Blue block crystals were filtered and washed with distilled water (60% yield based on W). Anal. Calcd for C$_{220}$H$_{384}$Cu$_{12}$N$_{132}$O$_{264}$P$_8$W$_{72}$ (23348.96): C 11.31, H 1.64, N 7.91. Found: C 11.28, H 1.66, N 7.95. IR (solid KBr pellet, cm^{-1}): 3742 (w), 3430 (s), 3131 (w), 2925 (w), 1644 (s), 1588 (w), 1524 (s), 1452 (s), 1381 (w), 1274 (m), 1218 (w), 1128 (m), 1082 (s), 953 (m), 919 (m), 789 (s), 635 (w), 513 (w).

Preparations of 1-, 2-, 3- and 4-CPEs. The compound **1** modified CPE (**1**-CPE) was fabricated as follows: 90 mg of graphite powder and 8 mg of **1** were mixed and ground together with an agate mortar and pestle to achieve a uniform mixture, and then 0.1 mL of Nujol was added with stirring. The homogenized mixture was packed into a glass tube with a 1.5 mm inner diameter, and the tube surface was wiped with paper. Electrical contact was established with a copper rod through the back of the electrode. In a similar manner, **2**-, **3**-, and **4**-CPEs were made with compounds **2**, **3**, and **4**.

X-ray Crystallographic Study. X-ray diffraction analysis data for compounds **1**−**4** were collected with a Bruker Smart Apex CCD diffractometer with Mo Kα (λ = 0.71073 Å) at 187 K. The structures were solved by direct methods and refined on F^2 by full-matrix least-squares methods using the *SHELXTL* package.[19] Some of the nonhydrogen atoms were refined isotropically because of the large unit cell volumes and relatively weak average intensities. For the compounds, all the hydrogen atoms attached to carbon atoms were generated geometrically while the hydrogen atoms attached to water molecules were not located but were included in the structure factor calculations. A summary of the crystallographic data and structural determination for them is provided in Table 1. Selected bond lengths and angles of the four compounds are listed in the Supporting Information Table S1. Crystallographic data for the structures reported in this paper have been deposited in the Cambridge Crystallographic Data Center with CCDC number 664324 for **1**, 664325 for **2**, 664326 for **3**, and 664328 for **4**.

Results and Discussion

Synthesis. Compounds **1–4** were synthesized under hydrothermal conditions. It deserves mention that the kind and

(18) Lyon, D. K.; Miller, W. K.; Novet, T.; Domaille, P. J.; Evitt, E.; Johnson, D. C.; Finke, R. G. *J. Am. Chem. Soc.* **1991**, *113*, 7209.

(19) (a) Sheldrick, G. M. *SHELXS-97, Program for Crystal Structure Solution*; University of Göttingen: Germany, 1997. (b) Sheldrick, G. M. *SHELXL-97, Program for Crystal Structure Refinement*; University of Göttingen: Germany, 1997.

Table 1. Crystal Data and Structure Refinements for Compounds **1–4**

	1	2	3	4
formula	$C_{21}H_{36}Cu_6N_{18}O_{65}P_2W_{18}$	$C_{24}H_{40}Cu_6N_{18}O_{64}P_2W_{18}$	$C_{48}H_{84}Cu_3N_{36}O_{68}P_2W_{18}$	$C_{220}H_{384}Cu_{12}N_{132}O_{264}P_8W_{72}$
fw	5332.9	5357	5815.09	23348.96
T (K)	187 (2)	187 (2)	187 (2)	187 (2)
cryst syst	triclinic	triclinic	monoclinic	monoclinic
space group	$P\bar{1}$	$P\bar{1}$	$C2/c$	$C2/c$
a (Å)	13.469(5)	13.0857(17)	14.649(5)	27.4420(13)
b (Å)	15.258(5)	17.004(2)	26.362(5)	15.9357(8)
c (Å)	20.189(5)	19.292(3)	29.960(5)	54.783(3)
α (°)	95.160(5)	82.128(2)		
β (°)	94.389(5)	86.703(2)	95.609(5)	102.6060(0)
γ (°)	107.452(5)	69.173(2)		
V (Å^3)	3919(2)	3974.2(9)	11514(5)	23380(2)
Z	2	2	4	2
D_c (g·cm^{-3})	4.514	4.473	3.347	3.312
μ (mm^{-1})	28.039	27.650	18.573	18.294
$F(000)$	4676	4708	10420	21008
final $R_1{}^a$, $wR_2{}^b$ [$I > 2\sigma(I)$]	0.0591, 0.1282	0.0861, 0.1916	0.0544, 0.1422	0.0580, 0.1085
final$R_1{}^a$, $wR_2{}^b$ (all data)	0.0929, 0.1436	0.1306, 0.2207	0.0616, 0.1484	0.0886, 0.1194
GOF on F^2	1.036	1.056	1.013	1.058

^{a} $R_1 = \Sigma||F_o|-|F_c||/\Sigma|F_o|$. ^{b} $wR_2 = \{\Sigma[w(F_o{}^2-F_c{}^2)^2]/\Sigma[w(F_o{}^2)^2]\}^{1/2}$.

the stoichiometry of the starting materials have a key role in the structural control of the self-assembly process. A different stoichiometry of btb/Cu resulted in different compounds **2** and **3**, whose structural difference will be discussed later. The ratio of btb to Cu is 1:11 for compound **2** and 1:17 for compound **3**.

The excess btb promoted the reduction of Cu^{II} to Cu^I (Scheme 1). Such a phenomenon is often observed in a hydrothermal reaction system containing N-donor ligand and Cu^{II}.[12d,20] This molar ratio influence on the oxidation state of copper ions also has been observed for the other two ligands btp and btx (Supporting Information Figure S1), although the crystal structures of the corresponding compounds were not obtained yet.

Description of the Crystal Structures. The α-[P$_2$W$_{18}$-O$_{62}$]$^{6-}$ (abbreviated to P$_2$W$_{18}$) anion is the inorganic building block in compounds **1–4**, which contains two [α-A-PW$_9$O$_{34}$]$^{9-}$ units derived from the α-Keggin anion by removal of a set of three corner-shared WO$_6$ octahedra.[21] The P–O and W–O lengths are in the normal ranges. To present clearly the crystal structures, all the coordination sites of P$_2$W$_{18}$, coordination numbers, modes of L (L = btp, btb, and btx) and copper ions, and Cu–L frameworks in compounds **1–4** are summarized in Table 2.

Crystal Structure of Compound 1. Crystal structure analysis reveals that compound **1** consists of six Cu^I ions, three btp ligands, one P$_2$W$_{18}$ anion, and three water molecules (Figure 1).

The Cu1, Cu3, and Cu5 ions are four-coordinated by two O atoms from two P$_2$W$_{18}$ anions and by two N atoms from two btp ligands in a "seesaw" style. The bond distances and angles around the copper ions are 1.882(18)–1.94(2) Å for Cu–N, 2.224(14)–2.77(17) Å for Cu–O, 163.9(8)–173.4(9)°

for N–Cu–N, 86.63(7)–105.66(7)° for N–Cu–O, and 82.09(4)–142.59(5)° for O–Cu–O, comparable to those in the four-coordinated Cu^I complexes.[7f,16i,22] The Cu6 ion also is four-coordinated by two O atoms and by two N atoms to form a distorted tetrahedron, but the two N atoms are from one btp ligand. The bond distances and angles around the Cu6 ion are 1.973(19), 1.979(18) Å for Cu–N, 2.089(16), 2.159(14) Å for Cu–O, 124.19° for N–Cu–N, 88.9(6)–122.2(7)° for N–Cu–O, and 93.36° for O–Cu–O. The Cu2 and Cu4 ions are both three-coordinated as follows: Cu2 by one O$_W$ atom and by two N atoms from one btp ligand, and Cu4 by one O atom from one P$_2$W$_{18}$ anion and by two N atoms from two btp ligands in a slightly distorted T-type coordination mode. The bond distances and angles around the Cu2 and Cu4 are 1.874(18)–1.94(2) Å for Cu–N, 1.92(2)–2.49(6) Å for Cu–O$_W$/O, 122.2(9)–166.9(8)° for N–Cu–N, and 92.56–120.4(8)° for N–Cu–O$_W$/O.

A notable feature in the structure of **1** is that the btp ligand exhibits flexible coordination modes with its four donor N atoms: (i) It acts as a tetradentate linkage bridging four Cu^I ions in a "H"-style to achieve the structural extension. (ii) It acts as a bidentate linkage, using two N atoms to bridge two Cu^I ions, while it provides the remaining two N atoms to chelate a Cu^I ion, which terminate the dimensional extension. The combination of the two coordination modes results in the formation of 1D ladder-like chains, in which the tetradentate bridging btp ligands are the "middle rail" of the ladder and the hexanuclear [Cu$_6$(btp)$_4$]$^{6+}$ circuit is the basic motif of the chains (Figure 2a). The ladder-like chains arrange parallel. The bis(triazole) ligands with such interesting coordination modes are rare in POM systems.

Also interesting is the 3D structure of compound **1**, where each P$_2$W$_{18}$ anion acts as a nine-connected linkage surrounded by four sets of the 1D chains, and each chain also is surrounded by four sets of the P$_2$W$_{18}$ anions. The P$_2$W$_{18}$ anion offers four terminal O atoms and two bridging O atoms to connect three chains (the purple, brown, and blue ones in

(20) (a) Wu, C.-D.; Lu, C.-Z.; Zhuang, H.-H.; Huang, J.-S. *Inorg. Chem.* **2002**, *41*, 5636. (b) Liu, C.-M.; Zhang, D.-Q.; Zhu, D.-B. *Cryst. Growth Des.* **2005**, *5*, 1639. (c) Sha, J.-Q.; Peng, J.; Liu, H.-S.; Chen, J.; Dong, B.-X.; Tian, A.-X.; Su, Z.-M. *Eur. J. Inorg. Chem.* **2007**, 1268.

(21) (a) Wang, J.-P.; Zhao, J.-W.; Niu, J.-Y. *J. Mol. Struct.* **2004**, *697*, 191. (b) Lu, Y.; Xu, Y.; Li, Y.-G.; Wang, E.-B.; Xu, X.-X.; Ma, Y. *Inorg. Chem.* **2006**, *45*, 2055.

(22) Felices, L. S.; Vitoria, P.; Gutiérrez-Zorrilla, J. M.; Lezama, L.; Reinoso, S. *Inorg. Chem.* **2006**, *45*, 7748.

Table 2. Coordination Sites of POM, Coordination Numbers, Modes of L (L = btp, btb, and btx) and Copper Ions, and Cu–L Frameworks in Compounds **1**–**4**
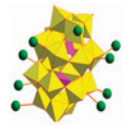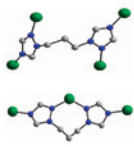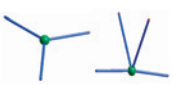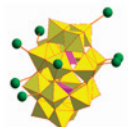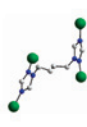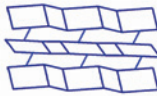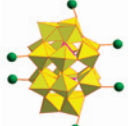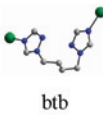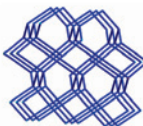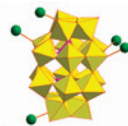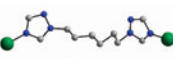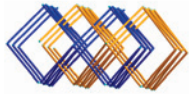
	coordination site of POM	coordination number and mode of L	coordination number and mode of copper ions	Cu-L framework
1		btp		
2		btb		
3		btb		
4		btx		

Figure 2b) by sharing only one side of each ladder-like chain, and it offers two bridging O atoms and one terminal O atom to link the fourth chain (the yellow one in Figure 2b) by sharing both sides of the chain. This is the first example of a polyoxoanion acting as a nine-connected linkage, which also is the highest connected POM ligand found up to now, to our knowledge.

Crystal Structure of Compound 2. Compound **2** consists of six Cu^I ions, three btb ligands, one P_2W_{18} anion, and two water molecules (Figure 3).
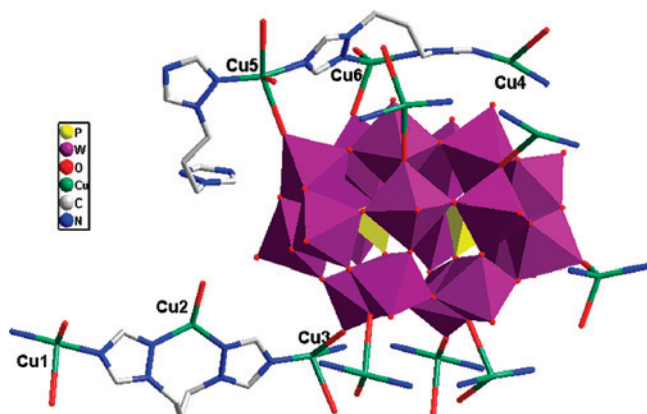

Figure 1. Stick/polyhedral view of the asymmetric unit of **1** and the coordination sites of the P_2W_{18} anion. The hydrogen atoms and crystal water molecules are omitted for clarity.

There are three types of coordination configurations for the six Cu^I centers: (i) The Cu1, Cu2, Cu3, and Cu5 atoms adopt the "seesaw" geometry, coordinated by two N atoms from two btb ligands and two O atoms from the two P_2W_{18} anions. (ii) The Cu4 atom adopts the T-shaped geometry, coordinated by two N atoms from two btb ligands and one O atom of the P_2W_{18} anion. (iii) The Cu6 atom adopts the linear geometry, coordinated by two N atoms from two btb ligands. The coexistence of three types of coordination geometries for Cu^I ions is seldom seen.[7f,23] The bond distances and angles are similar to those in **1**.

Different from the btp ligand in **1**, the btb molecule in compound **2** acts as a tetradentate bridging ligand in a single coordination mode, that is, the four N atoms coordinate to four Cu^I ions, to extend the MOF to a 2D net (Figure 4a, left). The net is composed of three kinds of circuits: dinuclear, tetranuclear, and hexanuclear $[Cu_n(btp)_n]^{n+}$ ($n =$ 2, 4, and 6) circuits (see Supporting Information Figure S2). The grid layers are wave-like when viewed along the b axis (Figure 4a, right).

The metal-organic polymeric layers are parallel to each other along the b axis, and the two adjacent layers are covalently connected by ennead-dentate P_2W_{18} anions, leading to a 3D structure (Figure 4b). Each P_2W_{18} anion offers

(23) Liu, C.-M.; Zhang, D.-Q.; Zhu, D.-B. *Cryst. Growth. Des.* **2006**, *6*, 524.
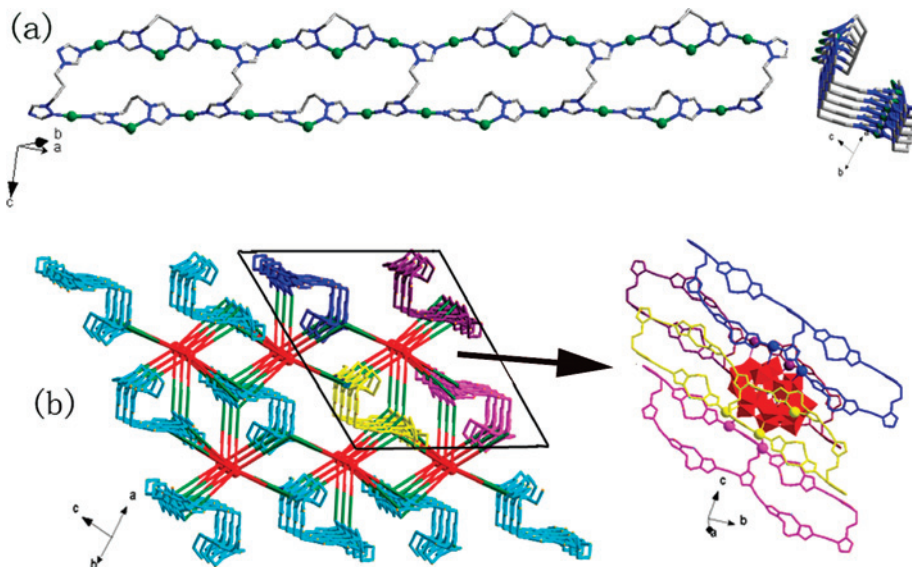
Figure 2. (a) Representation of the 1D Cu−btp polymeric chain in **1** consisting of hexanuclear $[Cu_6(btp)_4]^{6+}$ circuits along the given directions. Cu^I ion: green ball. (b) The 3D framework of **1** constructed from parallel chains connected by P_2W_{18} anions (red balls) and the detailed coordination environment of the anion (polyhedra).
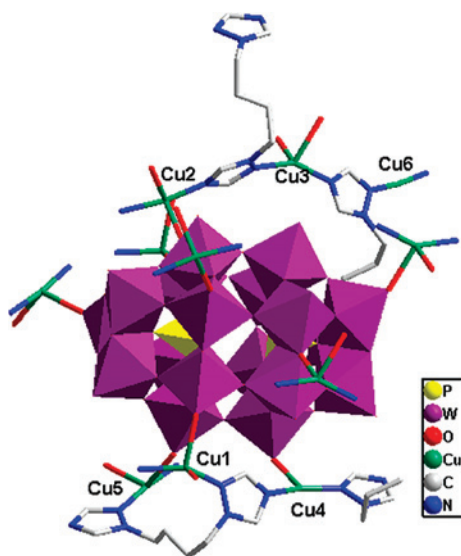

Figure 3. Stick/polyhedral view of the asymmetric unit of **2** and the coordination sites of the P_2W_{18} anion. The hydrogen atoms and crystal water molecules are omitted for clarity.

five terminal and one bridging O atom to link one layer (the green one in Figure 4b) and offers two terminal O atoms and one bridging O atom to link the other layer (the orange one in Figure 4b), which is sandwiched just like in a "hamburger". The wave-like MOF and POM layers are alternately arranged. Notably, viewing along the *a* axis, it can be found that the polyoxoanions only insert between the hexanuclear circuits of the layers (Supporting Information Figure S3), and the adjacent layers, like "quilts", overlay the P_2W_{18} anions. This selective insertion is probably due to the larger void of the hexanuclear circuits than of those of the others that accommodate the POM anions.

Crystal Structure of Compound 3. Compound **3** consists of three Cu^{II} ions, six btb ligands, one P_2W_{18} anion, and six water molecules (Figure 5). Each Cu^{II} ion is six-coordinated by four N atoms from four btb ligands and two O atoms

from two P_2W_{18} anions. The bond distances and angles around Cu^{II} ions are 1.979(11)−2.039(12) Å (Cu−N), 2.342(8)−2.433(8) Å (Cu−O), 88.5(5)−92.2(4)° (N−Cu−N), and 82.4(4)−96.9(4)° (N−Cu−O), which are similar to those in the six-coordinated copper(II) complexes.[7d]

In compound **3**, each btb molecule acts as a bidentate ligand linearly linking two Cu^{II} ions through the N atoms, while each Cu^{II} ion is coordinated by four btb ligands. Taking Cu^{II} ions as four-connecting nodes, a $4^2 \cdot 6^2 \cdot 8^2$ (Schläfli symbol) 3D MOF is generated (Cu1−Cu2, 7.68, 11.408 Å; Cu2−Cu2, 8.451, 8.542 Å, Figure 6a). In this open framework, quadrate and hexagonal channels arrange alternately along the *a* axis. The P_2W_{18} anions acting as hexadentate ligands incorporate only into the hexagonal channels, as shown in Figure 6b, which is expected for the big space of the hexagonal channel. The quadrate channels, unoccupied by P_2W_{18} anions, contain water molecules.

Crystal Structure of Compound 4. Compound **4** consists of three Cu^{II} ions, five and a half btx ligands, one P_2W_{18} anion, and four water molecules (Figure 7). Cu1 is five-coordinated by four N atoms of four btx ligands and one O atom of a P_2W_{18} anion in a square pyramidal geometry, having a τ value of 0.09 ($\tau = (\beta - \alpha)/60$),[24] with the angles N1−Cu1−N13, 171.72° (β) and N6−Cu1−N7, 166.17° (α). The Cu2 center is in a distorted octahedral geometry, defined by four N atoms from four btx ligands and two O atoms from two P_2W_{18} anions. Cu3 is six-coordinated by three N atoms of three btx ligands, two O atoms of one P_2W_{18} anion, and one water molecule. The coordination mode of the btx ligand is similar to that in compound **3**, and the bond distances and angles are also comparable to those in compound **3**.

In compound **4**, Cu1, Cu2, and Cu3 ions are viewed as three, four, and three connecting nodes, respectively, with the adjacent Cu−Cu distances of 13.149 Å (Cu1−Cu2),

(24) Addison, A. W.; Rao, T. N. *J. Chem. Soc., Dalton Trans.* **1984**, 1349.
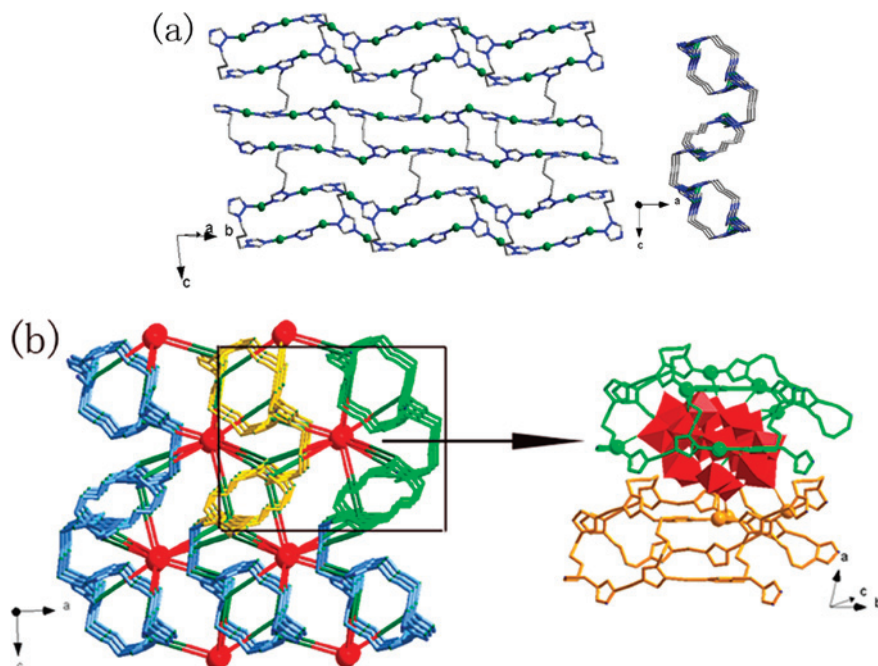
Figure 4. (a) Representation of the Cu−btb polymeric net in **2**: left, along the *a* axis; right, along the *b* axis. Cu^I ion, green ball. (b) The 3D framework of **2** constructed from parallel wave-like layers connected by P_2W_{18} anions (red balls) along the *b* axis and the detailed coordination environment of the anion (polyhedra).
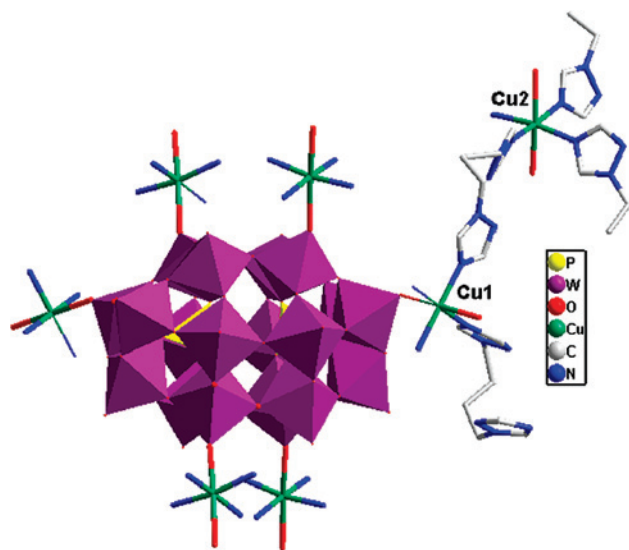

Figure 5. Stick/polyhedral view of the asymmetric unit of **3** and the coordination sites of the P_2W_{18} anion. The hydrogen atoms and crystal water molecules are omitted for clarity.

15.220 Å (Cu1−Cu3), 11.764 Å (Cu1−Cu1), 10.327 Å (Cu2−Cu2), and 15.451 Å (Cu2−Cu3). Thus, a $(6^1 \cdot 10^2)_2$-$(6^1 \cdot 8^2 \cdot 10^3)$ 3D MOF is formed. Interestingly, there exist two sets of $(6^1 \cdot 10^2)_2(6^1 \cdot 8^2 \cdot 10^3)$ 3D nets, which generate a 2-fold interpenetrated structure, as shown in Figure 8a. The P_2W_{18} anion, acting as a five-connected ligand, offers three terminal O atoms to link one net (the orange one in Figure 8b) and offers two terminal O atoms to link the other net (the blue one in Figure 8b). Thus, the two interpenetrated MOFs are united by the P_2W_{18} anions to construct a 3D POM coordination polymer structure.

Influence of the Flexible Bis(triazole) Ligands on the MOF Structures and Coordination Modes of the P_2W_{18} Anion. In this work, by changing the length of the flexible bis(triazole) ligands, we have achieved the alteration of the spacer and steric hindrance of the organic ligands to observe their effect on the assembly of the POM coordination polymers.

Although both compounds **1** and **2** are 3D frameworks built upon nine-connected P_2W_{18} anions and Cu^I ions with similar coordination geometries, the MOF structures are distinctively different, which rests only on the –CH$_2$– spacer difference of the bis(triazole) ligands. The influence of spacer difference on the MOF structures is obvious. In compound **1**, the short –(CH$_2$)$_3$– spacer makes the btp molecule act as a chelate ligand to coordinate to a Cu^I center by using two terminal N donors, which otherwise will play an extension role acting as a bridging ligand. Thus, in compound **1**, half the amount of the btp ligands is tetradentate and half the amount of the btp ligands is bidentate, which combine together to generate an interesting ladder-like double-chain MOF. However, in compound **2**, the btb ligand with a –(CH$_2$)$_4$– spacer is too long to form stable chelate bonds with the Cu^I ion. It therefore acts as the tetradentate bridging ligand, leading to the 2D MOF nets.

Compounds **3** and **4** also are 3D frameworks built upon multiconnected P_2W_{18} anions and the same Cu^{II} ions with similar coordination geometries. But the bis(triazole) ligands have a different –(CH$_2$)$_n$– spacer, which influences the metal-organic framework. This embodies two aspects. First, it is possible that the 2-fold interpenetrated MOF structure of $(6^1 \cdot 10^2)_2(6^1 \cdot 8^2 \cdot 10^3)$ nets in compound **4** is caused by the btx molecules with a –(CH$_2$)$_6$– spacer, which is the longest one among the three bis(triazole) ligands. Second, the coordination number of the POM ligands decreases from six in compound **3** to five in compound **4**, that is, it seems that
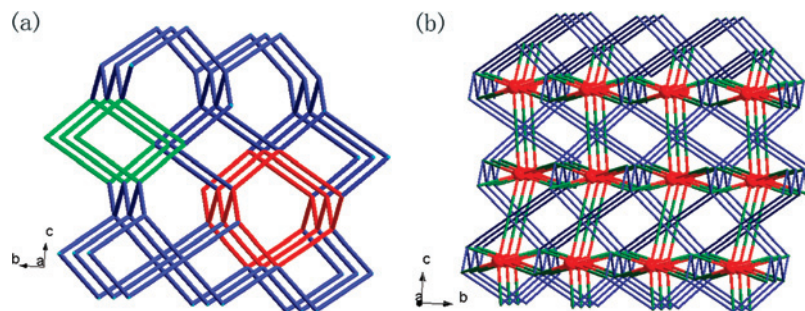
Figure 6. (a) Schematic diagram of the 3D MOF in **3** with quadrate (green) and hexagonal (red) channels arranging alternately. (b) The 3D framework of **3**, with the P_2W_{18} anions (red balls) incorporating only with the hexagonal channels.
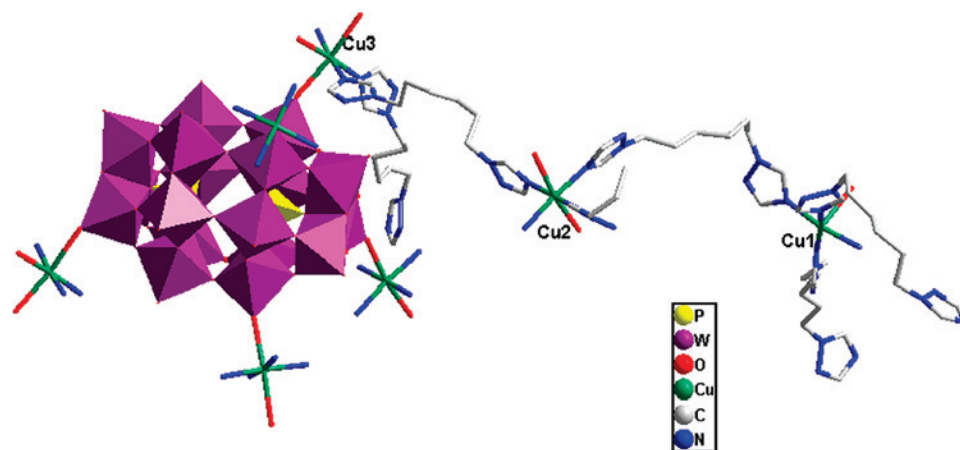

Figure 7. Stick/polyhedral view of the asymmetric unit of **4** and the coordination sites of the P_2W_{18} anion. The hydrogen atoms and crystal water molecules are omitted for clarity.
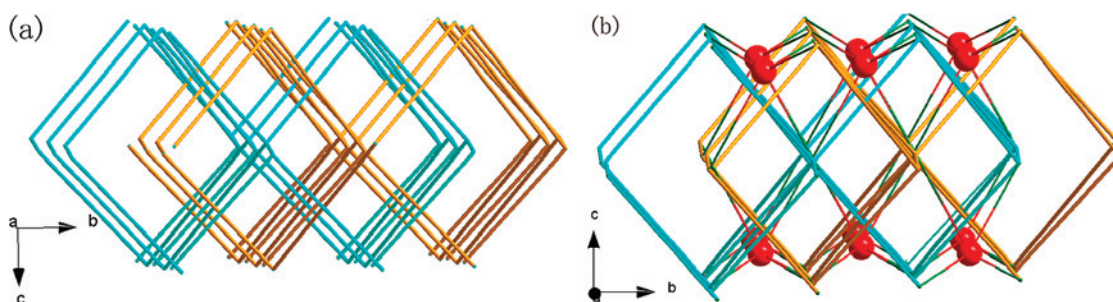

Figure 8. (a) Schematic view of the 2-fold interpenetrating network of the 3D MOF in **4**. (b) The 2-fold interpenetrating Cu−btx network linked by P_2W_{18} anions (red balls) to construct a 3D framework.

the longer the $-(CH_2)_n-$ spacer of the bis(triazole) ligands, the fewer the coordination sites provided by the P_2W_{18} anions. This is a consistent tendency observed in the four compounds, which is explicable considering the bigger steric hindrance of the flexible organic ligand with a longer $-(CH_2)_n-$ spacer. The decreasing molecular densities from 4.514 for compound **1** to 3.312 for compound **4** could also support this conclusion.

Usually, in the structural system of Wells-Dawson POM coordination polymers, the coordination sites provided by the P_2W_{18} anions are less than 5.[16,17] However, the coordination numbers of the P_2W_{18} anions in compounds **1–4** are from 5 to 9, and the coordination modes of the POMs are diversified. In compounds **1** and **2**, the P_2W_{18} anions act as nine-connected linkers to coordinate to the Cu^I ions through five terminal O atoms and four μ_2-bridging O atoms for **1** and through seven terminal O atoms and two μ_2-bridging O

atoms for **2**; in compounds **3** and **4**, the P_2W_{18} anions act as six- and five-connected linkers, respectively, to coordinate to the Cu^{II} ions. It is notable that the donor O atoms of the P_2W_{18} anions are all terminal oxygen atoms, likely because of the Cu^{II} ions arranged in octahedral and square pyramidal geometry. The coordination modes of the P_2W_{18} anions in compounds **1–4** are schematically summarized in Table 2. It is interesting to closely look into the environments of the POM anions (Figure 9). The POM anions are surrounded by four Cu−btp chains in compound **1**, sandwiched by two adjacent Cu−btb layers in compound **2**, and entrapped in the 3D Cu−btb framework in compound **3**, respectively. However, in compound **4**, the POM anions are entangled by the interpenetrated 3D Cu−btx framework, where the btx ligand is the longest one. In this case, given the big steric hindrance of the btx molecules, it is expected that the number
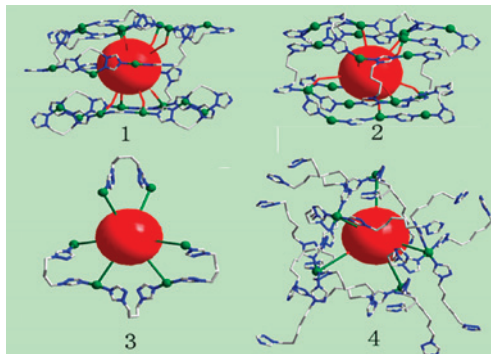
Figure 9. Schematic representations of the environments close to the POM anions in **1**-**4**, showing details of the Cu−L MOF motifs around the POM anions (green balls, copper atoms; red balls, polyoxoanions).

of the Cu−btx units grafted on to the polyoxoanions is reduced to maintain the stability of the structure.

Influence of the Metal Ion Coordination Geometries on the MOF Structures. Compounds **2** and **3** have the same POM anions and btb ligands, but the Cu ions are in different oxidation states. As is known, the Cu^I ions usually adopt versatile coordination geometries such as linear, "seesaw", and T-shaped coordination environment, as it does in the case of compound **2**; the Cu^{II} ions are prone to adopt the octahedral coordination geometry, and the Cu^{II} ions in compound **3** are solely in an octahedral coordination geometry. It is obvious that their different structures rely on the coordination habit of the Cu ions. Furthermore, these differences also induce different coordination behaviors of the P_2W_{18} anions in these compounds.

The flexible bis(triazole) ligands, with four donor N atoms as potential coordination nodes, also exhibit attractive coordination modes in compounds **1**–**4** with the coordination number ranging from 2 to 4, which is scarce compared with other bis(triazole)-containing POM coordination polymers.[12c,d] The diversity of the coordination modes of the flexible bis(triazole) ligands themselves deserves more attention. The coordination modes of the bis(triazole) ligands in compounds **1**–**4** are schematically summarized in Table 2.

In summary, the lengths of the bis(triazole) ligands and the coordination modes of the Cu ions have a synergic influence on the MOF dimensions and on the enveloping of the POMs through the Cu−L motifs.

FT-IR Spectra and XRPD Patterns. The IR spectra of compounds **1**–**4** are shown in the Supporting Information Figure S4. In the spectra of **1**–**4**, characteristic bands at 1089, 955, 905, and 773 cm^{-1} for **1**, 1088, 954, 911, and 778 cm^{-1} for **2**, 1090, 953, 905, and 782 cm^{-1} for **3**, and 1082, 953, 919, and 789 cm^{-1} for **4** are attributed to $\nu(P-O)$, $\nu(W=O)$, and $\nu(W-O-W)$, respectively. Bands in the regions of 1698−1140 cm^{-1} for **1**, 1685−1147 cm^{-1} region for **2**, 1631−1128 cm^{-1} for **3**, and 1644−1128 cm^{-1} for **4** are attributed to the btp, btb, and btx ligands.

The XRPD patterns for compounds **1**–**4** are presented in the Supporting Information Figure S5. The diffraction peaks of both simulated and experimental patterns match well in

key positions, indicating thus the phase purities of compounds **1**–**4**.

TGA. The TGA experiments were performed under a N_2 atmosphere with a heating rate of 10 °C·min^{-1} in the temperature range of 25−800 °C shown in Supporting Information Figure S6. The TG curves of compounds **1**–**4** show two distinct weight loss steps: The first weight loss step below 300 °C corresponds to the loss of water molecules. The second weight loss step is ascribed to the loss of organic molecules, 14% (calcd 13.91%) for **1**, 11.79% (calcd 12.13%) for **2**, 21.78% (calcd 22.27%) for **3**, and 22.68% (calcd 23.19%) for **4,** in the range of 300–800 °C.

Differential thermal analyses (DTA) give the decomposition temperatures (DT) of compounds **1**–**4**, 409 °C for **1**, 403 °C for **2**, 340 °C for **3**, and 331 °C for **4**, all higher than 300 °C, whereas the transition metal coordination polymers with similar flexible bis(triazole) ligands, for example, $\{[Mn(btb)(H_2O)_4](NO_3)\ _2\}_n$ (DT < 300 °C),[25] and noncovalently modified POM coordination polymers, for example, $[Cu^{II}(L)_2(H_2O)_2][Cu^I_2(L)_2]PMo_{12}O_{40}$ (DT < 250 °C),[12d] are all thermally less stable. Thus, one can find that the high connective Wells-Dawson POM coordination polymers have a higher thermal stability possibly owing to the robust P_2W_{18} linkages.

The DTA data show that compounds **1** and **2** are more stable than **3** and **4**. This can be explained by the characteristics of the structures/connectivity of the four compounds. In compounds **1** and **2**, the P_2W_{18} anions act as nine-connected linkers to coordinate to the Cu^I ions, and there are a total of four potential coordination sites of the bis(triazole) ligands to be utilized (Table 2.). However, in compounds **3** and **4**, the P_2W_{18} anions act as six- and five-connected linkers, respectively, to coordinate to the Cu^{II} ions. Furthermore, the btb and btx molecules provide two coordination sites (Table 2.). Both the connectivity of the POMs and the coordination sites of the ligands in compounds **1** and **2** are more than those in compounds **3** and **4**, which results in the tighter connectivity and packing modes in compounds **1** and **2**. The molecular densities, about 4.5 for compounds **1** and **2** and about 3.3 for compounds **3** and **4**, could also support this conclusion, namely, that for a similar POM coordination polymer species, the higher the connectivity is, the more stability it has.

Cyclic Voltammetry. Redox properties of compounds **1**–**4** were studied in 1 M H_2SO_4 aqueous solution. The electrochemical behaviors of the **1**–, **2**–, **3**–, and **4**–CPE (Supporting Information Figure S7) are similar except for some slight potential shift, and the behavior of **1**−CPE has been taken as an example. The cyclic voltammograms for **1**–CPE at different scan rates are presented in Figure 10 in the potential range of +600 to –700 mV. There exist three reversible redox peaks II–II′, III–III′, and IV–IV′ with the half-wave potentials $E_{1/2} = (E_{pa} + E_{pc})/2$ at –85(II–II′), –315.5(III–III′), and –541(IV–IV′) mV (scan rate: 80mV·s^{-1}), respectively. The redox peaks II–II′, III–III′, and IV–IV′ correspond to three

(25) Liu, X.-G.; Ge, H.-Y.; Zhang, Y.-M.; Hu, L.; Li, B.-L.; Zhang, Y. *J. Mol. Struct.* **2006**, *796*, 129.
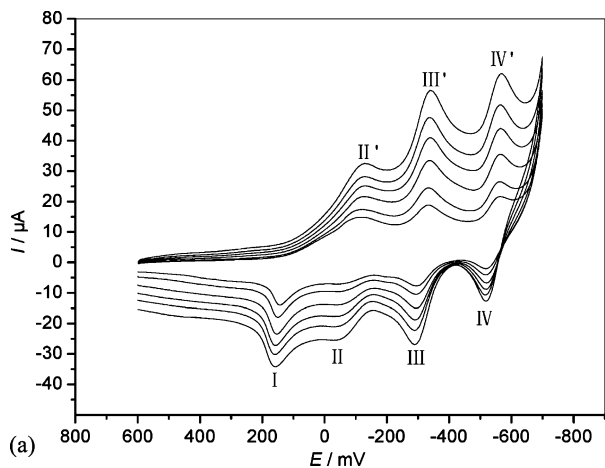
Figure 10. Cyclic voltammograms of the **1**–CPE in 1 M H_2SO_4 at different scan rates (from inner to outer: 80, 120, 200, 280, 360, and 480 mV·s^{-1}).

consecutive two-electron processes of the W centers.[26] In addition, the irreversible anodic peak I with the potential of +143 mV is assigned to the oxidation of the copper centers.[20c,27]

Furthermore, when the scan rates were varied from 80 to 480 mV·s^{-1} for **1**-CPE, the peak potentials change gradually: the cathodic peak potentials shift toward the negative direction and the corresponding anodic peak potentials shift toward the positive direction with increasing scan rates.

The Supporting Information Figure S8 shows cyclic voltammograms for the electrocatalytic reduction of nitrite at a bare CPE and a **1**-CPE in 1 M H_2SO_4 aqueous solution. No obvious voltammetric response is observed at a bare CPE in 1 M H_2SO_4 aqueous solution containing 12 mM nitrite in the potential range from 0.6 to –0.7 V. At the **1**-CPE, with the addition of nitrite, all three reduction peak currents gradually increase while the corresponding oxidation peak currents decrease, suggesting that nitrite is reduced by two-, four-, and six-electron reduced species of P_2W_{18} anions. It was also noted that the six-electron-reduced species presented the largest catalytic activity.

Conclusion

In this paper, four new compounds based on the highest connected P_2W_{18} anions and flexible bis(triazole) ligands have been synthesized under hydrothermal conditions. In these compounds, both the P_2W_{18} anion and the flexible bis(triazole) ligands exhibit rich coordination modes. Two important factors are found to influence the assembly of POM-based coordination polymers: (i) The steric hindrance of the organic ligand can influence the MOFs and tune the coordination mode of the polyoxoanion. (ii) The metal ion coordination geometries also have influence on the MOF structures. This work shows the perspective of using flexible ligands to construct the Wells-Dawson POM-based MOF polymers with interesting structure and to achieve the smart coordination sites of the Wells-Dawson type anions. Furthermore, this work extends the area of introducing flexible organic ligands into the POM system to obtain architectures where rigid inorganic frameworks and flexible metal coordination polymeric matrices are fused. The compounds **1**–**4** reflect this robustness/flexibility property. Notably, both $Cu^{I/II}$ ions and multidentate POMs can be viewed as unsaturated metal centers uniformly distributed in the architectures. It is possible that the catalytic, spectral, and electrochemical properties are tuned or improved by these active centers. The next challenge is the physical functionalization of these architectures through the dynamic properties of the frameworks, the alternative transition-metal oxidation states, and the changeable coordination sites provided by Wells-Dawson POMs. Further investigations are underway.

Supporting Information Available: Table of selected bond lengths and bond angles and XPRD, IR, TG, CV data, and structural figures for compounds **1**–**4** (PDF). This material is available free of charge via the Internet at http://pubs.acs.org.

IC7023082

(26) (a) Sadakane, M.; Streckhan, E. *Chem. Rev.* **1998**, *98*, 219. (b) Xi, X.-D.; Dong, S.-J. *J. Mol. Catal. A: Chem.* **1996**, *114*, 257. (c) McCormac, T.; Fabre, B.; Bidan, G. *J. Electroanal. Chem.* **1997**, *425*, 49.

(27) (a) Keita, B.; Abdeljalil, E.; Nadjo, L.; Contant, R.; Belgiche, R. *Electrochem. Commun.* **2001**, *3*, 56. (b) Jabbour, D.; Keita, B.; Nadjo, L.; Kortz, U.; Sankar Mal, S. *Electrochem. Commun.* **2005**, *7*, 841.